North-Holland

Strange-particle production in $\bar{p}$Xe annihilation at rest and at 0.4–0.9 GeV/c

V.V. Barmin, V.G. Barylov, G.V. Davidenko, V.S. Demidov, A.G. Dolgolenko, V.M. Golubchikov, V.A. Matveev, A.G. Meshkovsky, G.S. Mirosidi, A.N. Nikitenko, V.A. Shebanov, N.N. Shishov, B.S. Volkov, N.K. Zombkovskaja, A.D. Andrjakov, E.V. Demidova, V.A. Ergakov and Yu.V. Trebukhovsky

Institute of Theoretical and Experimental Physics, Moscow 117259, Russian Federation

C. Guaraldo

Laboratori Nazionali di Frascati dell'INFN C.P. 13, I-00044 Frascati, Italy

J. Cugnon and J. Vandermeulen

Université de Liège, Physique Nucléaire Théorique, Institut de Physique au Sart Tilman, Bâtiment B.5., B-4000 Liège 1, Belgium

Received 22 April 1992

Abstract: From a sample of 20 000 $\bar{p}$Xe annihilations obtained in the bubble chamber DIANA a search has been made for strange-particle production at rest and in flight (0.4–0.9 GeV/c) taking advantage also of the unique capability of the chamber to detect neutral (photon) channels. Inclusive features such as Λ, K^0_s and Σ^0 (the first time for the last particle) rates are presented, together with momentum and rapidity distributions. Semi-inclusive double-strangeness final states ΛKX, ΣKX and $K\bar{K}X$ are also presented. The observation of almost all strange channels allowed one to deduce the effective total strangeness content which turned out to be $(6.2 \pm 0.9)\%$. The K/π ratios, together with the mean multiplicities of protons, $\pi^{\pm}$ and π^0 mesons associated or not to strangeness production are also given. The results have been compared with a modified version of the standard intranuclear cascade model obtaining, within the model uncertainties, a good agreement under the assumption that the produced hyperons have no further nuclear interaction (no elastic scattering and no sticking).

E NUCLEAR REACTIONS ^{131}Xe($\bar{p}$, X), E at rest and in flight (0.4–0.9 GeV/c); measured strangeness and double-strangeness production, proton and pion mean multiplicities. Comparison with intranuclear cascade model. Bubble chamber.

1. Introduction

The production of heavy flavours is more and more the object of experimental studies in hadron–nucleus collisions and nucleus–nucleus collisions.

Specifically, strangeness production has been analyzed regarding such reaction mechanisms as the multiple-scattering effect [1]) and, at high temperatures and

Correspondence to: Prof. C. Guaraldo, INFN Laboratori Nazionali di Frascati, P.O. Box 13, I-00044 Frascati, Italy.

densities, as a signature of a phase transition leading to a quark-gluon plasma [2]). In this framework, the specific properties of antinucleons, in particular the dominant phenomenon of annihilation, in which all the valence quarks and valence antiquarks annihilate at distances of the order of the proton scale delivering relevant energy, offer ample possibilities for studying nuclear-matter excitation processes. Recently, Rafelski [3]) considered the possibility of formation of supercold quark matter in some of the data obtained in $\bar{p}$Ta annihilation [4]) at 4 GeV/c. Indeed other calculations based on the intranuclear cascade model [5]) and on the relativistic hydrodynamic model [6]) point out the possibility of reaching the condition of a phase transition already in the 4–6 GeV/c region.

The possibility of a less spectacular, although still unusual phenomenon, like the annihilation of an antiproton on two or more nucleons [7]) is demonstrated by the very existence of the $\bar{p}d \to \pi^- p$ reaction, recently measured by ASTERIX [8]) and OBELIX [9]) experiments at LEAR.

To study this potentially promising and new field of hadronic physics it is necessary to check the typical signature represented by strangeness enhancement. However, experimental data are scarce and not always complete in their main features. Concerning strange-particle production on targets heavier than deuteron, there have been essentially four published results: the KEK measurement of Miyano *et al.* [10]) [$\bar{p}$ + Ta at 4 GeV/c], the streamer chamber measurement of PS 179 experiment at LEAR [11]) [$\bar{p}$ + ^{3}He, ^{4}He, Ne, at rest and at 600 MeV/c], the measurement of Condo *et al.* [12]) [$\bar{p}$ + C, Ti, Ta, Pb at (0–450) MeV/c], the recent measurement of ASTERIX [8]) [$\bar{p}$ + ^{14}N at rest].

Along this line, this paper reports the new results on strange-particle production obtained with the Xe bubble chamber DIANA exposed to the 1 GeV/c antiproton beam of ITEP (Moscow). The results, at rest and in the (0.4–0.9) GeV/c interval, are the only ones, among the presently existing, in which also γ-rays have been measured revealing neutral decay channels of many particles. In particular, for the first time, an experimental value for the Σ^0 yield is given. The data have been fairly well fitted by a version of the intranuclear cascade model under the assumption of no further interaction (elastic scattering and sticking) of the hyperons after their formation.

2. Experimental procedure

This paper reports the results of the investigation of strange-particle production in the $\bar{p}$–Xe interaction at rest and at (0.4–0.9) GeV/c (average momentum about 0.7 GeV/c). The experiment was performed using the 700-liter xenon bubble chamber DIANA [13]). The chamber has dimensions $70 \times 70 \times 140$ cm^3, density of liquid xenon $\rho = 2.2$ g/cm^3, radiation length $X_0 = 3.7$ cm and was operating without a magnetic field. The chamber was exposed to a $\bar{p}$-beam with momentum of about 1 GeV/c: the data have been collected at 0.85, 0.95, 1.0, 1.05 and 1.1 GeV/c. The $\bar{p}$-beam was

obtained by irradiating a Be target with the proton beam of the ITEP 10 GeV proton synchrotron. The antiprotons were separated from negative secondaries by the double-stage CERN-ITEP separation system [14]). The intensity was chosen around 1–3 $\bar{p}$ per picture, within a momentum band of ~2%.

The data reported in this paper have been obtained making use of 2.5×10^4 pictures (out of a sample of 5×10^5 pictures), in which about 2×10^4 $\bar{p}$Xe inelastic interactions were found. Preliminary results concerning the analysis of 10^4 $\bar{p}$Xe annihilations have been reported in ref. [15]).

The antiprotons entering the chamber may annihilate in flight due to $\bar{p}$Xe interactions or, after energy dissipation due to ionization, annihilate at rest. The range distribution exhibits a typical smooth changing at the entrance of the chamber and a sharp bump in correspondence of annihilation at rest. In fig. 1a, the range distributions for an initial momentum of 0.95 GeV/c (solid line) and 1.1 GeV/c (dashed line) are shown. The position (R_0) of the experimental maximum corresponds to the calculated antiproton range in liquid xenon. In accordance with this distribution, we divided the annihilation events into two samples: the region of the peak, corresponding to annihilations at rest (the contamination of annihilation in flight is not more than 20%), and the region before the peak, where annihilations are in flight at momenta ranging from 0.4 up to 0.9 GeV/c.

The pictures were scanned looking for events with neutral strange-particle production. As candidates for neutral strange particles we considered: (a) "Vee"-events ($\Lambda \to \pi^- p$ and $K_s^0 \to \pi^+ \pi^-$); (b) three or four electron–positron pairs, produced by γ-quanta converted in xenon, which appeared to come from a single point inside the fiducial volume of the chamber ($K_s^0 \to 2\pi^0 \to 4\gamma$); and (c) two electron–positron pairs, produced by γ-quanta conversion and also directed to a single point in the chamber ($\Lambda \to \pi^0 n \to 2\gamma n$). We assumed as candidate origin for each event any $\bar{p}$Xe interaction situated close to the found candidate for the neutral strange particle. After inspection by physicists, all found candidates of $\Lambda \to p\pi^-$ and $K_s^0 \to \pi^+ \pi^-$ events were measured by means of stereoprojectors, which allowed one to reconstruct the spatial picture of the events to the chamber scale. For all candidates the angle of flight and the range of the secondaries were measured and the ionization of secondaries was evaluated. The energy of charged particles was obtained by range measurements. The photon energy was obtained by the total track length method. Details of the measurement procedure can be found in ref. [16]).

In order to obtain reliable identification of $\Lambda \to \pi^- p$ and $K_s^0 \to \pi^+ \pi^-$ events, the following selection criteria were applied:

(i) decay length of Vee's: $0.25 \leqslant R_V \leqslant 18.5$ cm;

(ii) opening angle of Vee's: $\theta_V \leqslant 150°$;

(iii) proton range: $R_p \geqslant 0.4$ cm ($P_p \geqslant 0.18$ GeV/c);

(iv) pion range: $R_\pi \geqslant 1.8$ cm ($P_\pi \geqslant 0.08$ GeV/c).

All the measured Vee-events were kinematically fitted to the hypothesis of a Λ-hyperon or a K_s^0 meson coming from the origin and decaying according to the

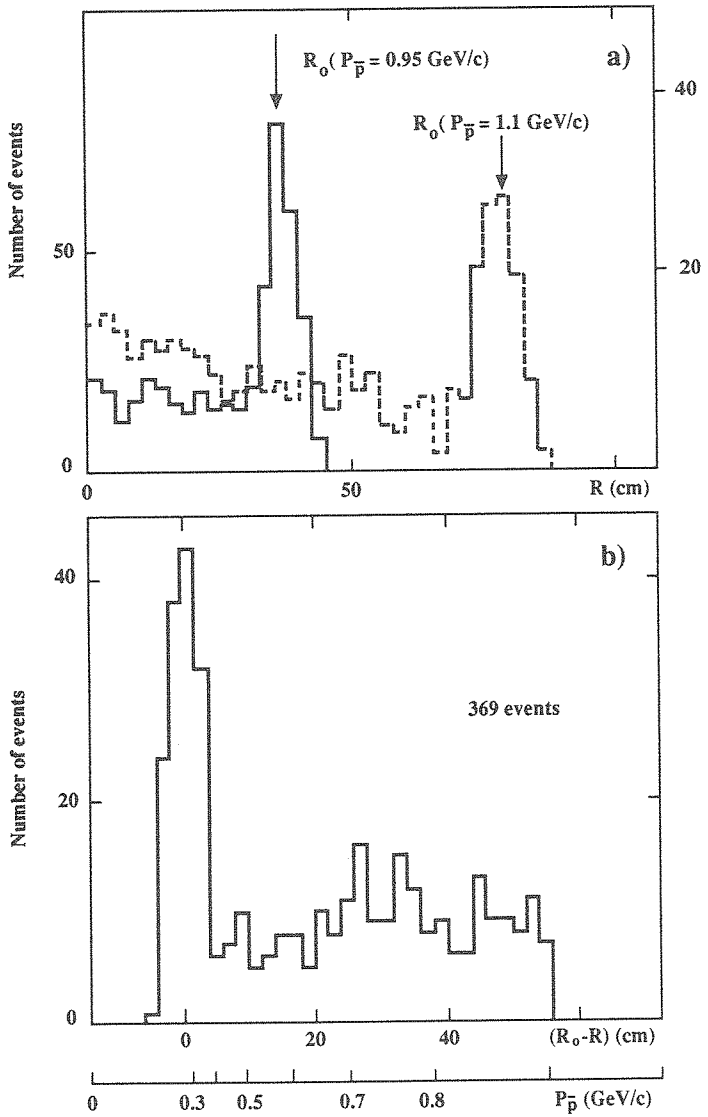

Fig. 1. (a) Range distributions in the Xe chamber of a 0.95 GeV/c (solid line) and 1.1 GeV/c (dashed line) antiproton beam: the position R_0 of the experimental maximum corresponds to the calculated range; (b) Λ and K_s^0 selected events distribution versus (R_0-R).

schemes $\Lambda \to \pi^- p$ and $K_s^0 \to \pi^+\pi^-$. After the fitting procedure, 369 annihilations accompanied by at least one Λ (Λ-momentum ≥ 0.15 GeV/c) or one K_s^0 were accepted. For each event the range difference (R_0-R) was calculated. The distribution of the 369 events versus (R_0-R) is reported in fig. 1b. The distribution is similar to that of fig. 1a and exhibits, as expected, a sharp peak at $(R_0-R)=0$.

According to our attribution, all events within the peak correspond to annihilations at rest, the remaining part of the spectrum corresponding to annihilations in flight.

The time-of-flight distributions of Λ and K_s^0 events are shown in fig. 2. The distributions are well described by a Monte Carlo calculation which takes into account the above selection criteria. Using the χ^2 procedure, the confidence levels turn out to be 74% and 91% for Λ and K_s^0, respectively.

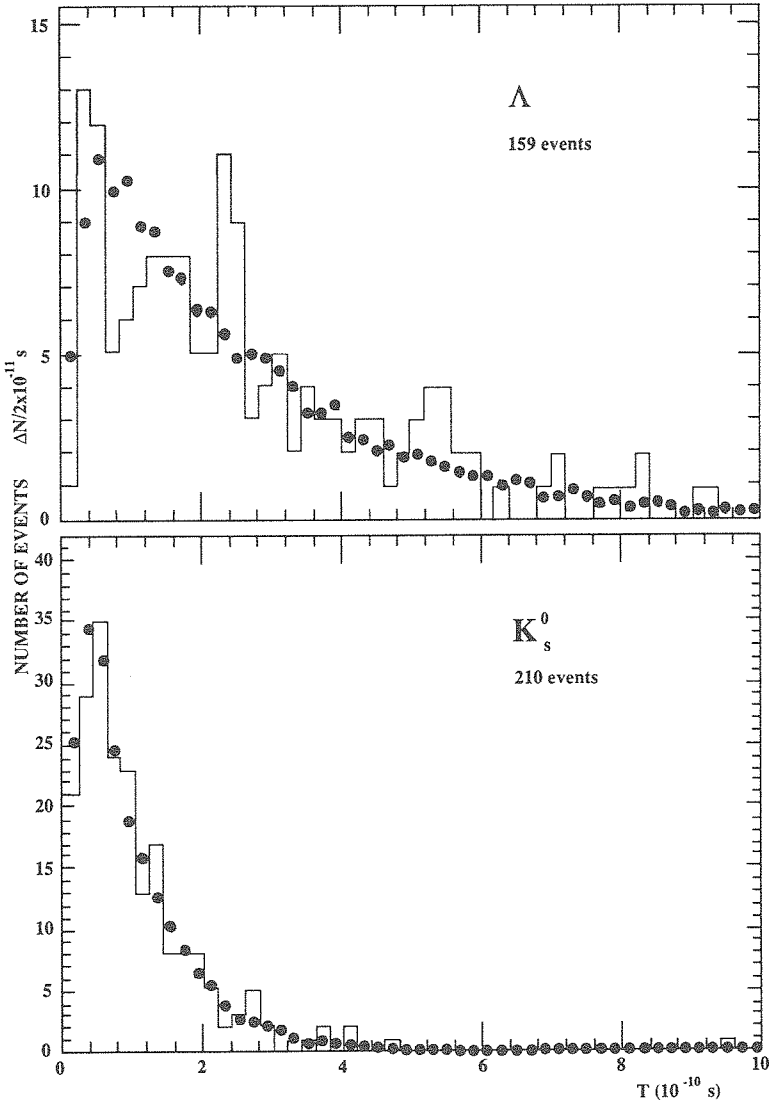

Fig. 2. Time-of-flight distributions of the Λ and K_s^0 selected events (histograms). Full circles: expected distributions from Monte Carlo calculation which takes into account the selection criteria.

3. Experimental results

Table 1 gives the number of measured events $\Lambda(\Sigma^0) \to \pi^- p$, $K_s^0 \to \pi^+\pi^-$ and $\Sigma^0 \to \Lambda\gamma$ at rest and at 0.4–0.9 GeV/c. The experimentally measured Σ^0 yields are the first ones to appear in literature. The notation $\Lambda(\Sigma^0)$ corresponds to the sum of Λ and Σ^0 events. We report this number in order to compare our data with those of the other experiments. In the table the data corrected for the detection efficiencies are also reported. These efficiencies took into consideration the experimental selection criteria and the correction for the unmeasured neutral decay modes $\Lambda \to \pi^0 n$ and $K_s^0 \to 2\pi^0$ [ref. [17])]. The correction factors turned out to be 3.32 and 1.92 for Λ and K_s^0 events, respectively. The values of Λ-yields compare rather well with the results of ref. [11]) (1.95 ± 0.43)% and with those of ref. [12]) (1.9 ± 0.4)% on complex nuclei in the same energy region.

It is interesting to note, as a check of the reliability of the values of the corrected events given in table 1, that starting from the measured Λ and K_s^0 in the charged decay channels (table 1), and taking into account the neutral branching ratios [17]), the scanning efficiencies (for 2γ-detection from $\Lambda \to n\pi^0$: 51%, and for $(3\gamma+4\gamma)$ from $K_s^0 \to 2\pi^0$: 59%) and the γ-detection efficiency of the Xe chamber (98%), the expected numbers for Λ and K_s^0 events in the neutral channels $\Lambda \to \pi^0 n$ and $K_s^0 \to 2\pi^0$ at rest and in flight turn out to be 99 and 70, respectively. These figures are in good agreement with the observed numbers for 2γ, and 3γ plus 4γ events, which are 113 and 73, respectively.

The $\Sigma^0 \to \Lambda\gamma$ events were obtained by taking into consideration 15 $\Lambda \to \pi^- p$ decays accompanied by a single γ pointing to the origin. The effective mass distribution of the events has a width which is in agreement with the experimental resolution and is peaked around the Σ^0 mass. To obtain the Σ^0 yield, correction for unmeasured Λ neutral decay mode was also taken into account.

TABLE 1

Inclusive strangeness production and total strangeness content in $\bar{p}$Xe annihilation at rest and in flight

Reaction	At rest			0.4–0.9 GeV/c		
	no. measured events	no. corrected events	yield (%)	no. measured events	no. corrected events	yield (%)
$\bar{p}Xe \to \Lambda(\Sigma^0)X$	59	196 ± 25	2.46 ± 0.30	111	372 ± 35	3.14 ± 0.30
$\bar{p}Xe \to K_s^0 X$	89	171 ± 18	2.14 ± 0.23	123	236 ± 21	1.99 ± 0.18
$\bar{p}Xe \to \Sigma^0 X$	3	13 ± 7.5	0.16 ± 0.09	12	45 ± 13	0.38 ± 0.11
$\bar{p}Xe \to$ anything		7975			11 843	
Total strangeness content			5.70 ± 0.50			5.90 ± 0.40

The observation of Σ^0 events allowed an evaluation of the total strangeness content in $\bar{p}$Xe annihilation. Under the assumptions $K_s^0 \simeq \frac{1}{4}(K+\bar{K})$ and $\Sigma^0 \simeq \frac{1}{2}\Sigma^{\pm}$, the total strangeness content S can be written as $S \simeq \frac{1}{2}[\Lambda(\Sigma^0)+2\Sigma^0+4K_s^0]$. The corresponding values turned out to be $(5.70 \pm 0.50)\%$ and $(5.90 \pm 0.40)\%$ for annihilation at rest and in flight, respectively.

In fig. 3, the K_s^0 and Λ momentum distributions for annihilations at rest and in flight are shown. The average momenta at rest are: $\langle P \rangle_{K_s^0}^{r} = 0.426$ GeV/c, $\langle P \rangle_{\Lambda}^{r} = 0.394$ GeV/c. The corresponding values in flight are: $\langle P \rangle_{K_s^0}^{f} = 0.431$ GeV/c, $\langle P \rangle_{\Lambda}^{f} = 0.443$ GeV/c, i.e. quite similar in the case of K_s^0 and 50 MeV/c shifted towards higher momenta for Λ's. In fig. 3 the momentum spectra at rest have been approximated by a Maxwell-Boltzmann distribution $dN/dp = A(p^2/E)\exp(-E/E_0)$, A and E_0 being experimental parameters. For Λ and K_s^0, the Boltzmann temperatures E_0 turned out to be 54 ± 9 MeV and 117 ± 15 MeV, respectively. The $E_0(\Lambda)$ value compares well with the corresponding values found by ASTERIX [8]) in deuterium and nitrogen (57 ± 6 and 62 ± 10 MeV, respectively). More generally, one can observe that the presently measured values of $E_0(\Lambda)$ and $E_0(K_s^0)$ are, within the errors, of the same order of the Boltzmann temperatures of protons and pions, respectively, emitted in antiproton annihilation on hydrogen and on complex nuclei [8]).

In fig. 4, the squared transverse momentum distributions of K_s^0 and Λ for annihilations in flight are presented. In the figure, the distributions have been fitted by an exponential function $dN/dp_\perp^2 = A\exp(-Bp_\perp^2)$ ($p_\perp^2 \leq 0.3$ (GeV/c)^2). The results of the fit are: $B(K_s^0) = (8.9 \pm 1.3)$ (GeV/c)$^{-2}$, $B(\Lambda) = (6.7 \pm 1.0)$(GeV/$c$)$^{-2}$. The B-parameters are in good agreement with the corresponding values obtained in $\bar{p}$Ta annihilation at 4 GeV/c [ref. [10])] (8.4 ± 0.4 and 7.3 ± 0.4 (GeV/c)$^{-2}$ for K_s^0 and Λ, respectively).

In fig. 5, the rapidity distributions of K_s^0 and Λ in $\bar{p}$Xe annihilation in flight are reported. The mean rapidity values are also given. The mean values of K_s^0 and Λ rapidity distributions at rest have been found compatible with zero ($\langle y \rangle_{K_s^0} = 0.05 \pm 0.05$ $\langle y \rangle_{\Lambda} = 0.02 \pm 0.04$), as expected.

In this experiment, due to the large volume of the Xe bubble chamber, there was a good efficiency for K^+ and $\Sigma^{\pm}$ identification by observing the decay modes $K^+ \to \mu^+\nu$, $\pi^+\pi^0$, $\pi^+\pi^+\pi^-$, $\pi^+\pi^0\pi^0$ and $\Sigma^{\pm} \to \pi^+ n$, $\pi^0 p$, $\pi^- n$. The K^- mesons were also identified by observing the secondary process of Λ-production: $K^- + Xe \to \Lambda + X$. Using a Monte Carlo calculation which took into account the experimental selection criteria, the detection efficiencies for K^+ and $\Sigma^{\pm}$ turned out to be around 80% and 40%, respectively. The K^- detection efficiency was taken equal to 25%, according to the result obtained in a dedicated run in which the Xe bubble chamber was exposed to a K^- beam. In this context, it was possible to observe, in a sample of events, the semi-inclusive double strangeness production. The results are reported in table 2. By analogy with table 1 and for the same numbers of annihilations at rest and in flight, the number of measured events, the number of events corrected for detection efficiencies and unobserved decay modes, and the yields of the corresponding semi-inclusive reactions are reported. As far as the yields of K^+K^-X and

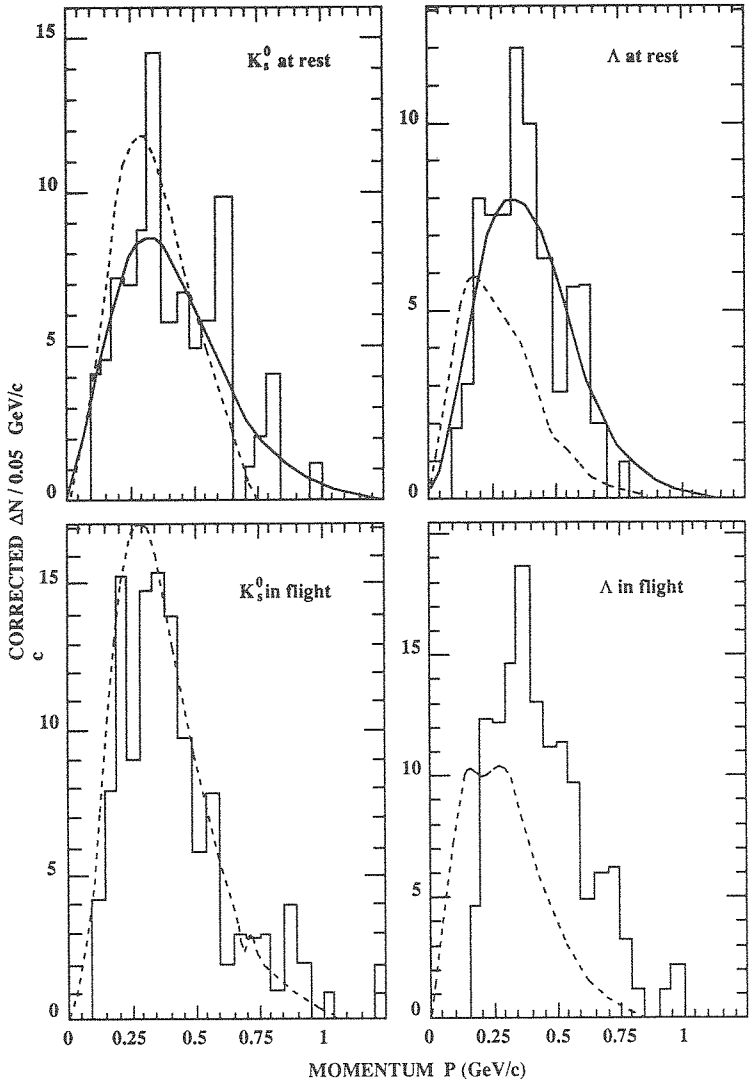

Fig. 3. K_s^0 and Λ momentum distributions for annihilations at rest and in flight (histograms). The solid lines are fits of the experimental data using Maxwell-Boltzmann distributions $dN/dp = A(p^2/E)\exp(-E/E_0)$ with $E_0(K_s^0) = 117 \pm 15$ MeV and $E_0(\Lambda) = 54 \pm 9$ MeV. The dashed lines are the predictions of the standard INC model [25]).

$K^+\Sigma^\pm X$ events, they were obtained in a special scanning of charged strange particles only.

The observation of almost all strange channels (except those with K_L^0) allowed, without making use of any additional assumption, to obtain the effective total strangeness content in $\bar{p}Xe$ annihilation. In summing the measured yields we took into account the weight of the channels with unobserved K_L^0 production. The effective

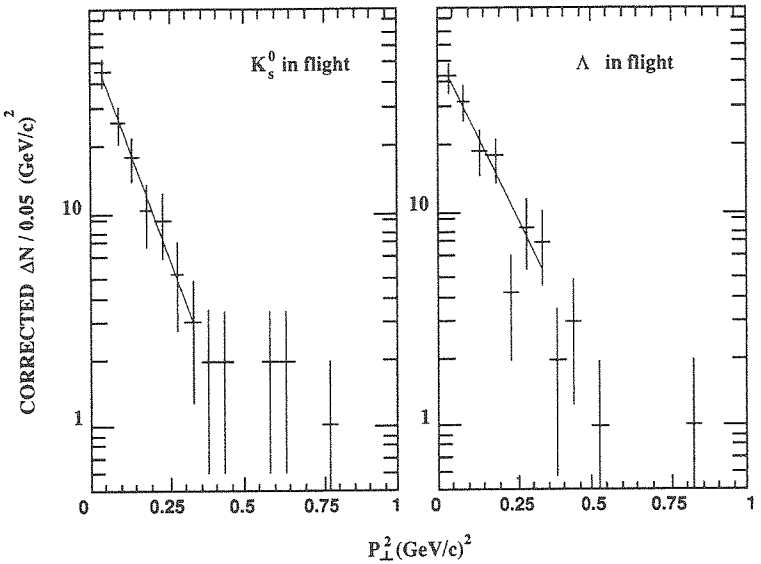

Fig. 4. Squared transverse-momentum distributions of K_s^0 and Λ after $\bar{p}$Xe annihilation in flight. The straight lines are fits of the experimental data with the function $dN/dp_\perp^2 = A \exp(-Bp_\perp^2)$ with $B(K_s^0) = 8.9 \pm 1.3$ (GeV/c)$^{-2}$ and $B(\Lambda) = 6.7 \pm 1.0$ (GeV/c)$^{-2}$ ($p_\perp^2 \leq 0.3$ (GeV/c)^2).

total strangeness content turned out to be independent of energy: $(6.20 \pm 0.90)\%$ and $(6.20 \pm 0.80)\%$ for annihilation at rest and in flight, respectively. It is interesting to observe that this value is not far, within errors, from the total strangeness produced in elementary annihilation at rest [18]).

Finally, in table 3 the measured K^-/K^+ ratio is reported. Within the large error, the absorption of K^- is higher than that of K^+, as expected. Using the data of table 2, and the results of the additional scanning of about 3000 $\bar{p}$Xe annihilations giving events with charged pions, it was possible to obtain the ratio of charged kaons to all charged pions. Moreover, although in this experiment it was not possible to distinguish π^+ from π^-, using the known ratio $\pi^+/\pi^- \simeq 0.7$, which remains practically the same in $\bar{p}$-nuclei annihilation from ^{20}Ne to ^{238}U [ref. [21])], also the K^+/π^- and K^-/π^- ratios were obtained. From the above additional sample, the average pion multiplicities $\langle N_{\pi^\pm} \rangle$ and $\langle N_{\pi^0} \rangle$ at rest and in flight, were obtained. The number of π^0's was reconstructed from the number of photons using the known γ-detection efficiency. The charged-pion multiplicity at rest $\langle N_{\pi^\pm} \rangle$ is in agreement with the value found in uranium [2.47 ± 0.09, ref. [19])]. Also $\langle N_{\pi^0} \rangle$ is in good agreement with the uranium data of ref. [20]) (1.36 ± 0.09).

The ratio $\Lambda(\Sigma^0)/K_s^0$ is reported in table 3.

Table 3 gives also the mean multiplicities of pions ($\pi^\pm$ and π^0) and protons, associated to strange-particle production. To obtain these values, only events with two registrated strange particles ($K\bar{K}$ and $K\Lambda$) were considered. In fact, if only one strange particle is seen, it means that the other one decays near the origin and, so,

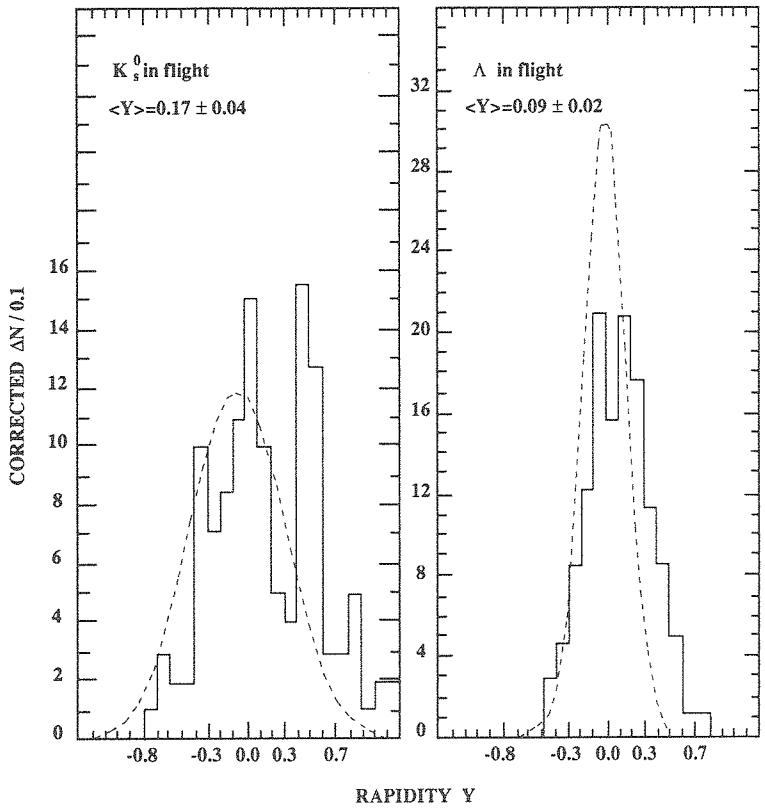

Fig. 5. Rapidity distributions of K_s^0 and Λ produced in $\bar{p}$Xe annihilation in flight (histograms) compared with standard INC model predictions [25]) (dashed lines).

TABLE 2

Semi-inclusive double strangeness production and effective total strangeness content in $\bar{p}$Xe annihilation at rest and in flight

Reaction	At rest			0.4–0.9 GeV/c			Weight for unobserved K_L^0
	no. measured events	no. corrected events	yield (%)	no. measured events	no. corrected events	yield (%)	
$\bar{p}Xe \to \Lambda(\Sigma^0)K_s^0X$	16	100 ± 25	1.25 ± 0.30	27	168 ± 32	1.42 ± 0.32	2
$\bar{p}Xe \to \Lambda(\Sigma^0)K^+X$	15	61 ± 16	0.76 ± 0.20	29	118 ± 22	1.00 ± 0.20	1
$\bar{p}Xe \to K_s^0K_s^0X$	6	22 ± 9	0.28 ± 0.11	6	22 ± 9	0.19 ± 0.08	4
$\bar{p}Xe \to K_s^0K^-X$	5	38 ± 17	0.48 ± 0.21	4	30 ± 15	0.25 ± 0.12	2
$\bar{p}Xe \to K_s^0K^+X$, $K_s^0\Sigma^\pm X$	7	19 ± 7	0.24 ± 0.08	13	31 ± 8.5	0.26 ± 0.07	2
$\bar{p}Xe \to K^+K^-X$, $K^+\Sigma^\pm X$	2[a])	6.5 ± 4.5	0.43 ± 0.30	5[a])	18 ± 8	0.55 ± 0.25	1
$\bar{p}Xe \to$ anything		7975			11843		
effective total strangeness content		6.20 ± 0.90			6.20 ± 0.80		

[a] These numbers have been obtained from a sample of 1519 at rest and 3302 in flight annihilation events.

TABLE 3

$K/\bar{K}$, K/π, Λ/K_s^0 ratios; pion and proton multiplicities with and without associated strangeness production in $\bar{p}Xe$ annihilation at rest and in flight

Ratio	At rest	0.4–0.9 GeV/c	Multiplicity	At rest	0.4–0.9 GeV/c
			$K\bar{K}$ tag		
K^-/K^+	0.83 ± 0.40	0.47 ± 0.19	$\langle N_p \rangle$	0.81 ± 0.14	1.38 ± 0.23
$K^+/\pi^\pm$	$(0.68 \pm 0.18)\%$	$(0.98 \pm 0.17)\%$	$\langle N_{\pi^\pm} \rangle$	0.84 ± 0.14	1.09 ± 0.19
$K^-/\pi^\pm$	$(0.56 \pm 0.23)\%$	$(0.45 \pm 0.17)\%$	$\langle N_{\pi^0} \rangle$	0.50 ± 0.10	0.41 ± 0.10
K^+/π^-	$(1.15 \pm 0.29)\%$	$(1.65 \pm 0.29)\%$			
			$K\Lambda$ tag		
K^-/π^-	$(0.95 \pm 0.39)\%$	$(0.76 \pm 0.28)\%$	$\langle N_p \rangle$	1.52 ± 0.18	2.47 ± 0.21
$\Lambda(\Sigma^0)/K_s^0$	1.15 ± 0.19	1.57 ± 0.20	$\langle N_{\pi^\pm} \rangle$	1.06 ± 0.13	1.13 ± 0.12
			$\langle N_{\pi^0} \rangle$	0.55 ± 0.08	0.55 ± 0.07
			$\langle N_p \rangle$	1.70 ± 0.08	2.70 ± 0.13
			$\langle N_{\pi^\pm} \rangle$	2.30 ± 0.12	2.08 ± 0.12
			$\langle N_{\pi^0} \rangle$	1.27 ± 0.07	1.08 ± 0.06

its secondaries may be taken into account in evaluating multiplicity, giving a wrong result. The following cuts on momenta were adopted in evaluating multiplicities: $P_{\pi^\pm} \geq 0.06$ GeV/c, $P_{K^\pm} \geq 0.14$ GeV/c, $P_p \geq 0.12$ GeV/c. It is worth noting in table 3 the substantial increase of the average proton multiplicity with $\bar{p}$-momentum both in $K\bar{K}$ and in $K\Lambda$ events.

The same increase of $\langle N_p \rangle$ with $\bar{p}$-momentum can be observed in $\bar{p}Xe$ annihilation events without any strange-particle tagging. The corresponding values are also reported in table 3.

4. Comparison with intranuclear cascade model predictions

It is well known that intranuclear cascade (INC) calculations can be considered, on the whole, successful in reproducing the general features of antinucleon–nucleus annihilation at low energy: see, for instance, refs. [21,22]). This essentially confirms the understanding of the underlying elementary multipion dynamics in nuclear matter. Beyond the standard versions of the INC code, more specific approaches have taken into account also the non-linear effect of the local reduction of nuclear density [23]) or have handled exactly charge conservation at each step of the cascade (in contradiction with the standard code, which disregards isospin degrees of freedom) [24]).

The strangeness production in antiproton annihilation on nuclei has been recently investigated by means of a cascade-type model, within the frame of the conventional picture of the annihilation on a single nucleon followed by subsequent rescattering proceeding in the hadronic phase [25]). Besides pions and nucleons, production and interactions of the following hadrons were introduced: K, $\bar{K}$, η, ω, Λ, $\bar{\Lambda}$, Σ and $\bar{\Sigma}$

and, as far as possible, the experimental reaction cross sections were used in the simulation. Specifically, the kaonic channel in $\bar{p}N$ annihilation was included; hyperon production was obtained through the pionic channel $\pi N \to YK$, the kaon rescattering $\bar{K}N \to Y\pi$, the ω-channel $\omega N \to YK$ and through hyperon strangeness exchange rescattering $\Lambda N \rightleftarrows \Sigma N$. Strangeness production induced by η's turned out to be only one tenth of that induced by ω's. Furthermore, around 600 MeV/c the strangeness production induced by three free pions was about the same as that induced by an η-particle. Therefore, the η-contribution could be considered as simulated by that of primordial pions.

The numerical results of this code compared relatively well with the experimental data up to 4 GeV/c, i.e. the $\bar{p}$Ta data at 4 GeV/c [ref. [10])], the CERN data on neon at 600 MeV/c [ref. [11])] and the AGS data on many targets (from C up to Pb) at (0–450) MeV/c [ref. [12])]. The rapidity distributions, the mass dependence, and the energy dependence relative to strangeness production were relatively well reproduced. The Λ-yield turned out to be in good agreement with experiment, while the K_s^0 yield appeared overestimated. One significant feature of the calculations was that the observed strangeness yields by no means required the introduction of exotic processes.

This version of the INC standard code including strangeness production [25]) was applied to the present sample of strange-particle events in $\bar{p}$Xe annihilation at rest and in flight. In fig. 3, the experimental momentum distribution of K_s^0 and Λ are compared with the model predictions both at rest and in flight (650 MeV/c). While K_s^0 distributions are rather well reproduced, the momentum distributions of Λ's are clearly not fitted by the model, which gives spectra systematically shifted towards low momenta. Also in the case of rapidity distributions of K_s^0 and Λ, shown in fig. 5, model predictions appear shifted towards the negative y-values.

In table 4, case (a), the calculated inclusive yields, at rest and in flight, of K_s^0, Λ and Σ^0 are compared with the corresponding experimental values. It appears evident that the Λ-yields are underestimated by about 60%, which roughly corresponds to the sticking probability of a hyperon.

Several possible changes of the standard cascade were possible at this point. There seemed no (reasonable) way to achieve agreement without demanding: (a) a small elastic scattering of hyperons, as clearly suggested from figs 3 and 5, and (b) a much smaller sticking probability for hyperons, as strongly suggested by the Λ-yield discrepancies.

As far as point (a) is concerned, this necessity already appeared clear in fitting the tantalum data at 4 GeV/c. It was indeed shown [see fig. 6 of ref. [25])] that the $y < 0$ part of the rapidity distribution was largely due to rescattering of Λ's and $\bar{K}$'s. A perfect agreement was obtained when the rescattering was totally suppressed. One has to distinguish between rescattering without strangeness exchange (basically elastic scattering $YN \to YN$) and rescattering with strangeness exchange ($\Lambda N \rightleftarrows \Sigma N$). We kept the rescattering with strangeness exchange, because we were

TABLE 4

Comparison between theory and experiment for strangeness yields in $\bar{p}$Xe annihilation at rest and in flight: (a) standard cascade [25]); (b) without hyperon elastic scattering; (c) without hyperon elastic scattering and sticking. In calculations the statistical uncertainty is not indicated, being smaller than the last significant figures for the average result

Momentum of $\bar{p}$ (GeV/c)	Type of calcul. and exp. value	Yields of particles (%)						Observed total strangeness (%)
		K	$\bar{K}$	K_s^0	Λ	$\Lambda(\Sigma^0)$	Σ^0	
at rest	(a)	5.8	3.2	2.3	1.41	1.52	0.11	5.4
	(b)	5.8	3.3	2.3	1.57	1.70	0.13	5.5
	(c)	5.8	3.3	2.3	1.90	2.10	0.20	5.8
	exp.			2.14 ± 0.23		2.46 ± 0.30	0.16 ± 0.09	6.0 ± 0.5
0.65	(a)	6.1	2.5	2.18	1.86	2.04	0.18	5.5
	(b)	6.1	2.4	2.10	2.23	2.48	0.25	5.7
	(c)	6.1	2.3	2.0	2.74	3.10	0.36	6.2
0.4–0.9	exp.			1.99 ± 0.18		3.14 ± 0.30	0.38 ± 0.11	6.0 ± 0.5

primarily interested in the strange-particle abundance (strangeness chemistry). We removed the elastic scattering, because it has a strong influence on the rapidity distribution of particles: experimental data indicate a small longitudinal slowing down of hyperons. As a secondary effect, removal of elastic scattering has a minor but not negligible effect on strangeness chemistry.

As far as point (b) is concerned, there is little doubt that the sticking probability has been overestimated in the standard cascade, but there is no experimental data which can constrain our description of the hyperon capture.

For purposes of illustration of the relevance of these effects, we performed a first calculation in which we forbid the elastic scattering of hyperons and a second one in which, in addition, we neglected also the possible sticking of hyperons. It is obvious, however, that the data can accommodate both a partial elastic scattering and a sticking probability between, say, 5–10%.

In figs. 6–8 the results of these new codes are shown. In fig. 6, the Λ momentum distributions at rest and in flight are better reproduced without hyperon elastic scattering with respect to the standard cascade (see fig. 3) and the agreement is rather good when also the sticking is totally suppressed. The Λ rapidity distribution in fig. 7 is well fitted by suppressing mainly the scattering, as underlined above. Finally, the calculated squared transverse momentum distribution takes the maximum advantage, as shown in fig. 8, when both scattering and sticking are suppressed.

In table 4, the two considered cases of suppression, no elastic scattering (case (b)), no scattering and no sticking (case (c)) are applied in evaluating the strange-particle yields. It is clear again that the absence of any hyperon interaction fits surprisingly well to the experimental data in both momentum intervals. In table 4

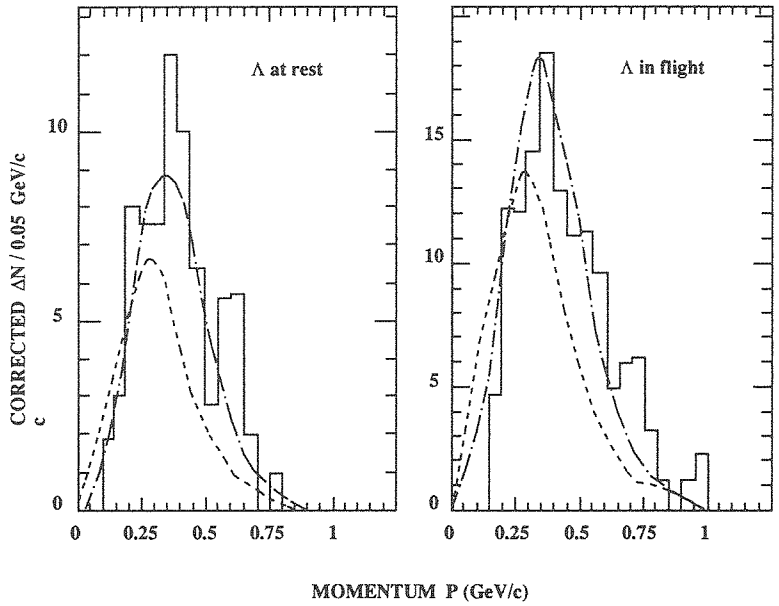

Fig. 6. Momentum distributions of Λ-particles produced in $\bar{p}$Xe annihilation at rest and in flight (histograms) compared with cascade model predictions. Dashed lines: standard cascade calculation [25]) without hyperon elastic scattering; dot-dashed lines: standard cascade calculation without hyperon elastic scattering and sticking.

is also reported the observed total strangeness content averaged from the values of table 1 and table 2, which turns out to be 6.0 ± 0.5 for both momentum intervals. The agreement of model (c) also with this quantity is indeed remarkable.

Finally, table 5 gives a comparison between the model prediction (case (c)) and the experimental values of pion and proton multiplicities associated or not to strangeness production, already contained in table 3.

There is a fairly good agreement between data and model as far as pion multiplicities are concerned. However, proton multiplicities represent a matter of disagreement between theory and experiment. In particular:

(1) in the experimental data, the ratio $\langle N_p \rangle_{flight}/\langle N_p \rangle_{rest}$ is roughly the same (1.6–1.7) for non-strange, $K\bar{K}$ and $K\Lambda$ events;

(2) the corresponding theoretical ratios are again the same for the three classes of events but systematically smaller (1.10–1.20) than the experimental ones;

(3) the theoretical multiplicities $\langle N_p \rangle$ are systematically smaller (with the only exception of $K\bar{K}$ events at rest) than the corresponding experimental ones.

Clearly, this discrepancy has nothing to do with strangeness production since, both theoretically and experimentally, there is no difference between the three classes of events. Writing:

$$\langle N_p \rangle = \langle N_\pi^{int} \rangle F, \tag{1}$$

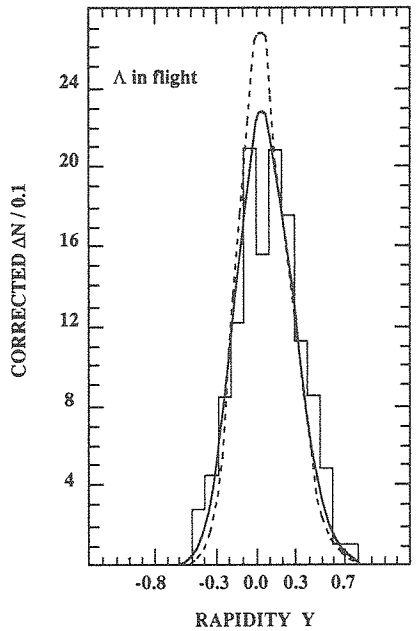

Fig. 7. Rapidity distribution of Λ-particles produced in $\bar{p}$Xe annihilation in flight (histogram) compared with cascade models predictions. Dashed line: standard cascade [25]) without hyperon elastic scattering; continuous curve: standard cascade without hyperon elastic scattering and sticking.

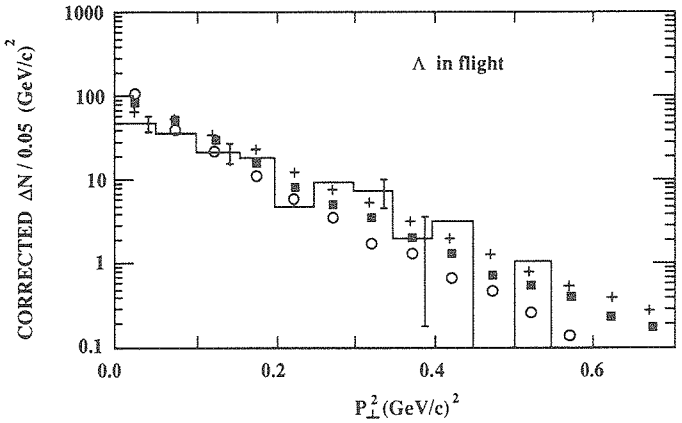

Fig. 8. Squared transverse momentum distribution of Λ-particles produced in $\bar{p}$Xe annihilations in flight (histogram) compared with cascade models predictions. Open circles: standard cascade [25]); black squares: standard cascade without hyperon elastic scattering; crosses: standard cascade without hyperon elastic scattering and sticking.

TABLE 5

Comparison between theory and experiment for proton and pion multiplicities associated or not to strangeness production. The cascade code is the standard of ref. [25]) without hyperon elastic scattering and sticking

Reaction	Multiplicity	At rest		In flight	
		experiment	model	experiment 0.4–0.9 GeV/c	model 0.65 GeV/c
$\bar{p}Xe \to K\bar{K}+X$	$\langle N_p \rangle$	0.81 ± 0.14	0.91 ± 0.01	1.38 ± 0.23	1.01 ± 0.01
	$\langle N_{\pi^\pm} \rangle$	0.84 ± 0.14	0.91 ± 0.01	1.09 ± 0.19	0.97 ± 0.01
	$\langle N_{\pi^0} \rangle$	0.50 ± 0.10	0.45 ± 0.01	0.41 ± 0.10	0.48 ± 0.01
$\bar{p}Xe \to K\Lambda+X$	$\langle N_p \rangle$	1.52 ± 0.18	1.03 ± 0.01	2.47 ± 0.21	1.26 ± 0.01
	$\langle N_{\pi^\pm} \rangle$	1.06 ± 0.13	1.13 ± 0.01	1.13 ± 0.12	1.07 ± 0.01
	$\langle N_{\pi^0} \rangle$	0.55 ± 0.08	0.56 ± 0.01	0.55 ± 0.07	0.53 ± 0.01
$\bar{p}Xe \to$ anything	$\langle N_p \rangle$	1.70 ± 0.08	1.31 ± 0.01	2.70 ± 0.13	1.49 ± 0.01
	$\langle N_{\pi^\pm} \rangle$	2.30 ± 0.12	2.26 ± 0.01	2.08 ± 0.12	2.15 ± 0.01
	$\langle N_{\pi^0} \rangle$	1.27 ± 0.07	1.13 ± 0.01	1.08 ± 0.06	1.08 ± 0.01

where $\langle N_\pi^{\text{int}} \rangle$ is the average number of interacting pions and F is the "efficiency" of a pion to eject a proton, the discrepancy may come from either $\langle N_\pi^{\text{int}} \rangle$, or F, or both. One can also write:

$$\langle N_\pi^{\text{int}} \rangle = \langle N_\pi^{\text{prim}} \rangle - \langle N_\pi^{\text{fin}} \rangle + \langle N_\pi^{\text{na}} \rangle , \tag{2}$$

where $\langle N_\pi^{\text{na}} \rangle$ is the number of interacting pions which are not absorbed.

Possible explanations of the discrepancy may come then from the following considerations:

(i) The calculation was performed for 650 MeV/c, whereas the experiment collects events from $\approx$0.4 up to $\approx$0.9 GeV/c. Data on $\bar{N}N$ interaction do not show practically any energy dependence; however, the annihilation site is deeper and deeper with increasing momentum. Anyway, the effect should not be large enough to account for the observed discrepancy.

(ii) F may be underestimated in the cascade. This may be due to the interaction of a single pion with several nucleons at a time, either because of quantum effects of the pion wave function or because the nucleons are acting cooperatively.

(iii) If one looks at eq. (2), one may also imagine that $\langle N_\pi^{\text{na}} \rangle$ has been underestimated. One can also imagine that $\langle N_\pi^{\text{prim}} \rangle$ is larger than in free space and that the absorption is larger than expected, thus keeping $\langle N_\pi^{\text{fin}} \rangle$ the same, which could explain the good agreement with the experimental pion multiplicities.

In other words, if the effect is real, it seems to point towards a larger overall pion "efficiency": in terms of number of interactions and of dynamics of the interaction. This is equivalent to a greater pion inelasticity, for some misunderstood reasons. Claiming for "true" multinucleon annihilations [7]) indeed does not help to find an explanation of the puzzle. $B = 1$ annihilations indeed increase the proton abundance.

However, they are mainly characterized by a strangeness enhancement beyond the values predicted by the cascade model, which does not occur in this case.

5. Conclusion

Strange-particle production in $\bar{p}$Xe annihilation at rest and at 0.4–0.9 GeV/c has been measured by the Xe bubble chamber DIANA exposed to the 1 GeV/c antiproton beam of the proton synchrotron of ITEP of Moscow. Inclusive strangeness rates of Λ, K_s^0 and Σ^0 have been obtained. The Λ-yields compare well with the value obtained in the experiments at AGS [12]) and at CERN [11]). The Maxwell–Boltzmann temperature of the Λ-source turns out to be the same found recently in nitrogen by ASTERIX [8]), while the B-parameters of the squared transverse momentum distributions of Λ and K_s^0 are very similar to the values found in $\bar{p}$Ta annihilation at 4 GeV/c [ref. [10])]. The Σ^0 yields at rest and in flight have been directly measured for the first time in this experiment. Semi-inclusive double strangeness production has been also measured, which represents the first observation in $\bar{p}$–nucleus annihilation of almost all strange channels (with the only exception of K_L^0 production). This allowed to obtain experimentally the effective total strangeness content of the reaction without any additional assumption. The obtained value can be substantially explained by conventional mechanisms, leaving scarce room for unusual $B=1$ annihilations, according to the model of ref. [7]). Charged- and neutral-pion multiplicities, both associated to events with strange particles and without strangeness, have been also measured and compare very well with the pion multiplicities measured in annihilation on heavy nuclei like uranium [19,20]). Attention has been given to the measurement of the K/π ratios. As far as the K^+/π^- ratio is concerned, which is an indicator of strangeness enhancement in nuclear matter, the value found at rest is smaller of about a factor 2 with respect to the corresponding values measured on many nuclei at CERN by the PS 183 experiment [26]).

The experimental results have been compared with a modified version of the intranuclear cascade code used to describe strangeness production [25]).

The results of our model are remarkably good. In particular, it allows to account for the observed very low value of the Σ^0/Λ ratio ($\approx$0.1), much smaller than previously suggested [27]). The results concerning momentum and rapidity distribution, individual strangeness yield and pion multiplicities are also remarkably good, at the expense, however, of the extreme assumption that the hyperon has no further interaction after its formation (no elastic scattering and no sticking). This typical "transparency" concerns only hyperons and not kaons. Whether some profound meaning is underlying this feature (something akin to colour transparency) cannot be presently decided, the model being not precise enough to really infer some definite conclusion. Moreover, it is certainly necessary to verify if these hypotheses can be applied also to other systems and therefore more experimental data on strangeness production on nuclei are certainly needed. By the way, as recalled above,

also the tantalum data at 4 GeV/c [ref. [10])] required, in order to be fitted, the same specific request to the conventional INC model [25]).

The authors wish to express their gratitude to Yu.A. Batusov, K.G. Boreskov, I.V. Falomkin, L.A. Kondratyuk and M.G. Sapozhnikov for useful discussions. They are also indebted to the staff of the ITEP proton synchrotron and to the separator and bubble chamber teams, which made the experiment possible. Finally, they thank the scanners, the measurers and the computing staff of ITEP for their efforts.

References

1) J. Randrup and C.M. Ko, Nucl. Phys. **A343** (1980) 519
2) J. Rafelski, Phys. Lett. **B91** (1980) 281;
J. Rafelski and B. Müller, Phys. Rev. Lett. **48** (1982) 1066;
P. Koch, J. Rafelski and W. Greiner, Phys. Lett. **B123** (1983) 151;
N. Glendenning and J. Rafelski, Phys. Rev. **C31** (1985) 823;
A. Shor, Phys. Rev. Lett. **54** (1985) 1122
3) J. Rafelski, Phys. Lett. **B207** (1988) 371
4) K. Miyano *et al.*, Phys. Rev. Lett. **53** (1984) 1725
5) D. Strottman and W.R. Gibbs, Phys. Lett. **B149** (1984) 288
6) A.A. Amsden *et al.*, Phys. Rev. **C15** (1977) 2059
7) J. Cugnon and J. Vandermeulen, Phys. Lett. **B146** (1984) 16
8) J. Riedlberger *et al.*, Phys. Rev. **C40** (1989) 2717
9) A. Adamo *et al.*, Proc. Int. Symp. on meson and light nuclei V, Prague, Sept. 1991
10) K. Miyano *et al.*, Phys. Rev. **C38** (1988) 2788
11) F. Balestra *et al.*, Phys. Lett. **B194** (1987) 192; Nucl. Phys. **A526** (1991) 415
12) G.T. Condo *et al.*, Phys. Rev. **C29** (1984) 1531
13) V. Barmin *et al.*, Prib. Techn. Exp. **4** (1984) 63 (in Russian)
14) V. Barmin *et al.*, ITEP report no. 99 (1977)
15) V. Barmin *et al.*, ITEP report no. 19-90 (1990);
A. Dolgolenko, *in* Low energy antiproton physics, ed. P. Carlson *et al.* (World Scientific, Singapore, 1991) p. 205
16) V. Barmin *et al.*, Sov. J. Nucl. Phys. **45** (1) (1987) 62
17) Particle Data Group, Phys. Lett. **B239** (1990) 1
18) R. Armenteros *et al.*, CERN report CERN/PSLL/80-101 (1980)
19) E.D. Minor *et al.*, Z. Phys. **336** (1990) 461
20) T.A. Armstrong *et al.*, Z. Phys. **332** (1989) 467
21) J. Cugnon and J. Vandermeulen, Ann. de Phys. **14** (1989) 49
22) C. Guaraldo, Nuovo Cim. **102A** (1989) 1137
23) Ye.S. Golubeva *et al.*, Nucl. Phys. **A483** (1988) 593
24) J. Cugnon, P. Deneye and J. Vandermeulen, Phys. Rev. **C38** (1988) 795
25) J. Cugnon, P. Deneye and J. Vandermeulen, Phys. Rev. **C41** (1990) 1701
26) G.A. Smith, *in* The elementary structure of matter, ed. J.M. Richard *et al.* (Springer, Berlin, 1988) p. 219
27) C.B. Dover and P. Koch, *in* Hadronic matter in collisions 1988, ed. J. Rafelski *et al.* (World Scientific, Singapore, 1989) p. 703